Crystal Structures of *Giardia lamblia* Guanine Phosphoribosyltransferase at 1.75 Å[†,‡]

Wuxian Shi,[§] Narsimha R. Munagala,[||] Ching C. Wang,[||] Caroline M. Li,[§] Peter C. Tyler,[⊥] Richard H. Furneaux,[⊥] Charles Grubmeyer,[@] Vern L. Schramm,*[,§] and Steven C. Almo*[,§]

Department of Biochemistry, Albert Einstein College of Medicine, 1300 Morris Park Avenue, Bronx, New York 10461, Department of Pharmaceutical Chemistry, University of California, San Francisco, California 94143, Carbohydrate Chemistry Team, Industrial Research Ltd., Lower Hutt, New Zealand, and Department of Biochemistry and Fels Research Institute, Temple University School of Medicine, Philadelphia, Pennsylvania 19140

Received January 20, 2000; Revised Manuscript Received March 20, 2000

ABSTRACT: *Giardia lamblia*, the protozoan parasite responsible for giardiasis, requires purine salvage from its host for RNA and DNA synthesis. *G. lamblia* expresses an unusual purine phosphoribosyltransferase with a high specificity for guanine (GPRTase). The enzyme's sequence significantly diverges from those of related enzymes in other organisms. The transition state analogue immucillinGP is a powerful inhibitor of HGXPRTase from malaria [Li, C. M., et al. (1999) *Nat. Struct. Biol. 6*, 582−587] and is also a 10 nM inhibitor of *G. lamblia* GPRTase. Cocrystallization of GPRTase with immucillinGP led unexpectedly to a GPRTase·immucillinG binary complex with an open catalytic site loop. Diffusion of ligands into preformed crystals gave a GPRTase·immucillinGP·Mg^{2+}·pyrophosphate complex in which the open loop is stabilized by crystal contacts. *G. lamblia* GPRTase exhibits substantial structural differences from known purine phosphoribosyltransferases at positions remote from the catalytic site, but conserves most contacts to the bound inhibitor. The filled catalytic site with an open catalytic loop provides insight into ligand binding. One active site Mg^{2+} ion is chelated to pyrophosphate, but the other is chelated to two conserved catalytic site carboxylates, suggesting a role for these amino acids. This arrangement of Mg^{2+} and pyrophosphate has not been reported in purine phosphoribosyltransferases. ImmucillinG in the binary complex is anchored by its 9-deazaguanine group, and the iminoribitol is disordered. No Mg^{2+} or pyrophosphate is detected; thus, the 5′-phosphoryl group is needed to immobilize the iminoribitol prior to magnesium pyrophosphate binding. Filling the catalytic site involves (1) binding the purine ring, (2) anchoring the 5′-phosphate to fix the ribosyl group, (3) binding the first Mg^{2+} to Asp125 and Glu126 carboxyl groups and binding Mg^{2+}·pyrophosphate, and (4) closing the catalytic site loop and formation of bound $(Mg^{2+})_2$·pyrophosphate prior to catalysis. Guanine specificity is provided by two peptide carbonyl oxygens hydrogen-bonded to the exocyclic amino group and a weak interaction to O6. Transition state formation involves N7 protonation by Asp129 acting as the general acid.

Giardia lamblia is a protozoan parasite that causes giardiasis in up to 20% of the world population, and is the most common protozoan disease in the United States (*1*, *2*). The symptoms of giardiasis include nausea, anorexia, fever, and severe diarrhea. Protozoan parasites are deficient in de novo purine synthesis and require purine salvage for survival. *G. lamblia* is an ancient member of the eukaryotes. Its purine salvage enzymes differ from those known from other protozoa. It therefore serves as a model for studying the development of purine metabolism in protozoa. Two purine salvage enzymes, guanine and adenine phosphoribosyltransferases (GPRTase and APRTase),[1] are present in *G. lamblia* and function to salvage purine bases for RNA and DNA synthesis (*3*).

G. lamblia GPRTase catalyzes the reversible Mg^{2+}-dependent transfer of the phosphoribosyl group from 5-phospho-α-D-ribosyl 1-pyrophosphate (PRPP) to guanine to form GMP (*4*; Figure 1). *Giardia* GPRTase has limited amino acid sequence homology to hypoxanthine/guanine/xanthine phosphoribosyltransferases (H/G/XPRTases) from other species, with only 23 and 21% of its sequence being identical to those of human and malarial HG(X)PRTases, respectively. However, the amino acids involved in substrate binding and

[†] Supported by NIH Grants GM41916 (V.L.S.), GM52125 (C.G.), and AI19391 (C.C.W.).

[‡] Coordinates for the X-ray crystal structures described here have been deposited at the RCSB structural database as file names 1DQP and 1DQN.

* Corresponding authors. Telephone: (718) 430-2813. Fax: (718) 430-8565. E-mail: vern@aecom.yu.edu or almo@aecom.yu.edu.

[§] Albert Einstein College of Medicine.

[||] University of California.

[⊥] Industrial Research Ltd.

[@] Temple University School of Medicine.

[1] Abbreviations: PRPP, 5-phospho-α-D-ribosyl 1-pyrophosphate; GPRTase, guanine-PRPP phosphoribosyltransferase; APRTase, adenine-PRPP phosphoribosyltransferase; immucillin-G, (1*S*)-1-(9-deazaguanin-9-yl)-1,4-dideoxy-1,4-imino-D-ribitol; immucillin-GP, immucillin-G 5′-phosphate; immucillin-H, (1*S*)-1-(9-deazahypoxanthin-9-yl)-1,4-dideoxy-1,4-imino-D-ribitol; immucillin-HP, immucillin-H 5′-phosphate; PP_i, inorganic pyrophosphate; HGPRTase, hypoxanthine/guanine-PRPP phosphoribosyltransferase; HGXPRTase, hypoxanthine/guanine/xanthine-PRPP phosphoribosyltransferase; DTT, dithiothreitol.

10.1021/bi000128t CCC: $19.00
Published on Web 05/16/2000

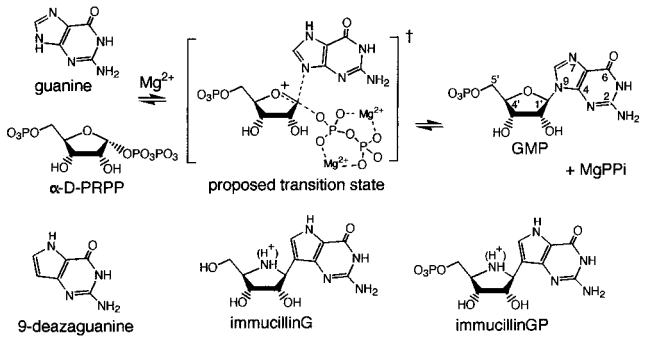

FIGURE 1: Reaction catalyzed by *G. lamblia* GPRTase, the proposed transition state, and the structures of 9-deazaguanine, immucillinG, and immucillinGP. Two features of the proposed transition state are incorporated into immucillinGP. The partial positive charge of the transition state ribooxocarbenium ion is mimicked by the iminoribitol (p$K_a \sim 6.5$; *22*). At the transition state, the pK_a of N7 of the purine ring increases. The equivalent position in immucillinGP has a pK_a of >8.

catalysis are highly conserved. *Giardia* GPRTase demonstrates a strong preference for guanine as a substrate. Humans express an adenine-specific and a hypoxanthine-guanine phosphoribosyltransferase, but no guanine-specific enzyme. Malarial purine salvage is attributed to a phosphoribosyltransferase using hypoxanthine, guanine, and xanthine as substrates. The *Giardia* enzyme exhibits a >1000-fold preference for guanine over hypoxanthine, and does not utilize xanthine as a substrate (*4*, *5*).

ImmucillinGP was designed to resemble the proposed transition state for phosphoribosyltransferases that use guanine as a substrate, and has been demonstrated to be a transition state analogue inhibitor for human and malarial HG(X)PRTases (*6*). Here, it is shown to be a powerful inhibitor of *Giardia* GPRTase (Figure 1). The structures of human and malarial HG(X)PRTases in complex with immucillins and Mg^{2+}·pyrophosphate have been determined recently, and reveal several features pertinent to transition state binding (*7*, *8*). We describe here two crystal structures of *Giardia* GPRTase, both refined to 1.75 Å resolution. The binary complex contains only immucillinG in the catalytic sites. Crystals of the binary complex were soaked with immucillinGP, Mg^{2+}, and PP_i to give crystals containing immucillinGP, two Mg^{2+} ions, and pyrophosphate in the catalytic site. These structures reveal that *Giardia* GPRTase has a distinctive hood subdomain compared to the other H/G/XPRTases (*7*−*12*). Comparison of the *Giardia* GPRTase·immucillinGP·Mg^{2+}·PP_i complex with other H/G/XPPRTases reveals unique structural features for substrate anchoring and suggests the mechanism for guanine specificity in the *Giardia* enzyme. One of the Mg^{2+} binding positions in the catalytic site has not been previously identified in related H/G/XPRTases. The fortuitous formation of the binary complex with immucillinG, and the crystal packing interactions that provide an ordered, fully occupied, but partially open catalytic site, gives structural evidence for the step-by-step filling of the catalytic site prior to catalysis.

MATERIALS AND METHODS

Expression and Purification of G. lamblia GPRTase. Recombinant *G. lamblia* GPRTase was overexpressed in *Escherichia coli* SØ606 (Δ*gpt-pro-lac, thi, hpt, Rec A*$^-$) as previously described (*4*). The cells were grown in low-phosphate minimal induction medium with MOPS salts supplemented with 0.2% glucose, 1.5 μM thiamine, 20 mg/L adenine, 0.2% Casamino acids (Difco), and an equimolar mixture of Na_2HPO_4 and NaH_2PO_4 (0.1 mM). Cell lysate was applied to a MonoQ column equilibrated with 0.1 M Tris-HCl (pH 7.8), 8 mM $MgCl_2$, and 1 mM DTT. The eluate was dialyzed against 25 mM CHES (pH 9.0), 8 mM $MgCl_2$, and 1 mM DTT and rechromatographed on a MonoQ column, equilibrated against CHES buffer at pH 9.0. Recombinant GPRTase that was >95% homogeneous was eluted with a linear gradient of 0 to 0.5 M KCl in the same buffer. To isolate the selenomethionyl GPRTase, the bacteria were grown in a modified induction medium. Instead of Casamino acids, selenomethionine (Sigma), Thr, Phe, Leu, Ile, Lys, Val, and Pro were added at concentrations of 0.1 g/L. The enzyme was isolated and purified from the cell lysate as described above. The presence of three selenomethionines in the purified enzyme monomeric subunit was confirmed by LC−MS, as predicted by the amino acid sequence. The initiating methionine was not present in the purified protein.

Synthesis of ImmucillinGP. ImmucillinGP was synthesized from 1,4-dideoxy-5-(*O-tert*-butydimethylsilyl)-1,4-imino-2,3-*O*-isopropylidene-D-ribitol as a starting material as described previously (*6*). The structure was confirmed by ^{13}C and ^{31}P NMR assignments.

Analysis of Phosphatase Activity. Trace amounts of phosphomonoesterase activity in preparations of *G. lamblia* GPRTase were detected by incubating the enzyme preparation at 1.5 mg/mL and 37 °C in the presence of 12 mM *p*-nitrophenyl phosphate in 50 mM Hepes (pH 8.1). Controls compared the rates of nonenzymatic solvolysis of *p*-nitrophenyl phosphate under the same conditions. The activity was detected by the release of the yellow *p*-nitrophenylate anion at 400 nm. Experiments could detect 1 part in 10^9 phosphomonoesterase molecules with respect to GPRTase activity. Phosphomonoesterase was detected at 1 part per 10^7 to 10^8 parts of GPRTase, and was sufficient to convert all immucillinGP to immucillinG in the crystallization drops in a period of several days at room temperature.

Inhibition Studies of GPRTase. Reaction rates were measured by the ultraviolet absorbance change at 257.5 nm as GMP is formed from guanine and 5-phosphoribosyl 1-pyrophosphate (PRPP). Assay mixtures contained 100 mM Tris-HCl (pH 7.4), 40 μM guanine, 1 mM PRPP, and 8 mM $MgCl_2$. The extinction coefficient for the reaction was determined to be 5900 M^{-1} cm^{-1} at 30 °C. ImmucillinGP and pyrophosphate were added as desired to establish the inhibition constant, K_i. Values of K_i were calculated from the relationship $v_s = v_o A/[K_m(1 + I/K_i) + A]$, where v_o is the uninhibited rate, v_s is the rate at various inhibitor concentrations, A is the substrate concentration, and I is the inhibitor concentration. Reaction conditions that give slow-onset inhibition required v_s to be measured from steady state rates after the slow onset period was complete (*13*).

Crystallization. G. lamblia recombinant selenomethionyl GPRTase was cocrystallized with a 1:1.1 stoichiometry of immucillinGP, 1 mM $MgCl_2$, and 1 mM sodium pyrophosphate, using hanging drop diffusion at 18 °C. Two microliters of a 10 mg/mL protein solution was mixed with an equal volume of the crystallization medium containing 20%

Table 1: Data Collection Statistics

	immucillinG complex	immcillinGP complex	Se remote	Se edge	Se peak
detector	MarCCD	MarCCD	Brandeis CCD	Brandeis CCD	Brandeis CCD
wavelength (Å)	0.979	0.979	0.9500	0.9789	0.9786
resolution (Å)[a]	1.75 (1.78−1.75)	1.75 (1.78−1.75)	2.4 (2.49−2.40)	2.5 (2.59−2.50)	2.5 (2.59−2.50)
no. of reflections					
total	210690	195866	124727	113806	95243
unique	50590	50789	20171	17619	17636
$I/(\sigma)I$	40.8 (20.2)	40.3 (17.8)	33.6 (15.5)	35.0 (17.9)	30.1 (15.1)
completeness (%)	98.9 (98.7)	99.5 (99.1)	99.1 (99.1)	99.6 (99.9)	98.7 (99.2)
R_{sym} (%)[b]	3.9 (7.5)	3.6 (8.2)	4.1 (7.3)	4.2 (6.6)	4.9 (7.5)
R_{anom} (%)[c]			3.1	3.0	4.4

[a] Values in parentheses are for the highest-resolution shell. [b] $R_{sym} = \Sigma_i|I_{hi} - \langle I_{hi}\rangle|/\Sigma_i|I_{hi}|$, where h specifies unique reflection indices and i specifies symmetry equivalent observations of h. [c] $R_{anom} = \Sigma_h|I_h^+ - I_h^-|/\Sigma_h|I_h^+ + I_h^-|$, where h specifies unique reflection indices.

polyethylene glycol 4000, 5% 2-propanol, and 100 mM HEPES at pH 7.5, and the mixture was equilibrated against 1.0 mL of the medium. After 3−8 weeks, small rod-shaped crystals grew to a maximum size of 0.1 mm × 0.1 mm × 0.3 mm. Diffraction from these crystals is consistent with space group $P2_12_12_1$ (a = 56.9 Å, b = 71.8 Å, and c = 123.5 Å) with a dimer in the asymmetric unit (V_m = 2.34 Å^3/Da, 47% solvent content).

Preparations of GPRTase contained trace amounts of alkaline phosphatase activity that resulted in the hydrolysis of immucillinGP to immucillinG and phosphate during crystallization. Electron density generated from the resulting crystals shows features corresponding to 9-deazaguanine, but not the iminoribitol or Mg^{2+}•pyrophosphate groups. Soaking the orthorhombic crystals in saturated immucillinGP containing 1 mM $MgCl_2$ and 1 mM sodium pyrophosphate for 10 h, followed by rapid freezing, resulted in electron density corresponding to the GPRTase•immucillinGP•Mg^{2+}•PP_i complex.

Data Collection and Processing. Multiwavelength anomalous dispersion (MAD) data were collected using a Brandeis CCD detector at beamline X12C (Brookhaven National Laboratory, Upton, NY). Crystals were sequentially dipped for 2 min in crystallization medium containing glycerol at concentrations of 5, 10, 15, and 20% (a total of 8 min) before rapid freezing in a nitrogen stream at −178 °C. MAD data to 2.5 Å resolution were collected from a single frozen crystal at the selenium dispersion peak (0.9786 Å), at the edge (0.9789 Å), and at a remote wavelength (0.9500 Å). Data were reduced and scaled using the DENZO package (*14*). Two high-resolution (1.75 Å) data sets for refinement of the GPRTase•immucillinG and GPRTase•immucillinGP•Mg^{2+}•PP_i complexes were collected at 0.979 Å wavelength using a Mar CCD detector at beamline X9B (Brookhaven National Laboratory) (Table 1).

Phasing. A total of six selenium sites were anticipated from the two GPRTase molecules in the asymmetric unit based on the amino acid sequence (excluding the N-terminal methionine). All six selenium sites were located by difference Patterson and cross-validation difference Fourier methods implemented in the SOLVE package. These gave an overall Z-score value of 41.7 and figure of merit of 0.37 using the data from 20 to 2.5 Å (*15*). Initial MAD phases were improved by solvent flattening and histogram matching using the program DM in the CCP4 package (*16*). The 2-fold noncrystallographic symmetry axis was located in the solvent-flattened map, and refined to a correlation coefficient of 0.48 using the RAVE package (*17*). After noncrystallographic averaging and solvent flattening using the program DM, the resulting map allowed for 80% of the sequence to be built using program O (*18*).

Structure Refinement. Refinement was implemented in the CNS suite (*19*) with anisotropic B correction, bulk solvent correction, simulated annealing refinement, and individual B factor refinement using high-resolution data for both GPRTase structures. The structure containing immucillinG was refined to R_{cryst} and R_{free} values of 20.4 and 23.2%, respectively, using 20−1.75 Å data. The final model includes residues 1−230 for each monomer, two 2-propanol molecules, 485 solvent molecules, and the 9-deazaguanine portion of immucillinG. The GPRTase•immucillinGP•Mg^{2+}•PP_i ternary complex was refined to 1.75 Å with R_{cryst} and R_{free} values of 20.4 and 23.4%, respectively. The model for one subunit of the dimer consists of residues 1−230, immucillinGP, pyrophosphate, and two Mg^{2+} ions. The other subunit is less ordered and contains residues 1−230, immucillinGP, pyrophosphate, and no well-ordered Mg^{2+} ions. The asymmetric unit contains a total of 476 water molecules and one 2-propanol molecule. Both structures demonstrate excellent stereochemistry with 100% of the amino acid residues in the most favored and additionally allowed structural regions, as determined by PROCHECK (*20*). Refinement statistics for both GRTase complexes are listed in Table 2.

RESULTS AND DISCUSSION

Inhibition of G. lamblia GPRTase by ImmucillinGP. Initial reaction rate studies indicated a K_i value of 60 ± 6 nM when immucillinGP was used as a competitive inhibitor with respect to Mg•PRPP. Under these conditions, normal initial rate kinetics were observed. The addition of 1 mM pyrophosphate permitted the formation of a more tightly bound inhibitory complex, and the K_i from initial rates decreased. A slow-onset phase resulting in an increased level of inhibition was clearly evident under these conditions. When the data are analyzed for the K_i^* value following slow-onset inhibition (*13*), the K_i value is 10 ± 2 nM.

Structure. The peptide folds in immucillinG, and immucillinGP•Mg^{2+}•PP_i complexes of *Giardia* GPRTase are similar but not identical. The monomer of GPRTase is folded into a single domain that can be further divided into two subdomains, designated the core and the hood (Figure 2a). The core subdomain of the GPRTase is similar to the cores observed in other PRTases structures and consists of a five-stranded parallel β-sheet (β2, 62−69; β3, 86−94; β5, 120−128; β6, 144−152; and β7, 167−174) surrounded by several

Table 2: Refinement Statistics for *G. lamblia* GPRTase Structures

	immucillinG complex	immucillinGP complex
space group	$P2_12_12_1$	$P2_12_12_1$
a (Å)	56.860	56.632
b (Å)	71.610	71.553
c (Å)	122.369	123.080
resolution (Å)	20.0−1.75	20.0−1.75
R_{cryst} (%)[a]	20.4	20.3
R_{free} (%)[b]	23.2	23.4
no. of reflections for refinement	45122	45295
no. of reflections for the free *R* calculation	5053	5080
no. of amino acid residues	460	460
ligands	2 immucillinG 2 2-propanol	2 immucillinGP 2 pyrophosphate 2 Mg^{2+} ions 1 2-propanol
no. of water molecules	485	478
rmsd from ideal		
bonds (Å)	0.008	0.007
angles (deg)	1.40	1.35
average *B* factor		
protein	19.4	19.8
ligand	24.0	28.5
water	27.8	28.3

[a] $R_{cryst} = \Sigma||F_o| - |F_c||/\Sigma|F_o|$ for all reflections, where F_o and F_c are the observed and calculated structure factors, respectively. [b] R_{free} was calculated against 10% of the reflections removed at random from the refinement.

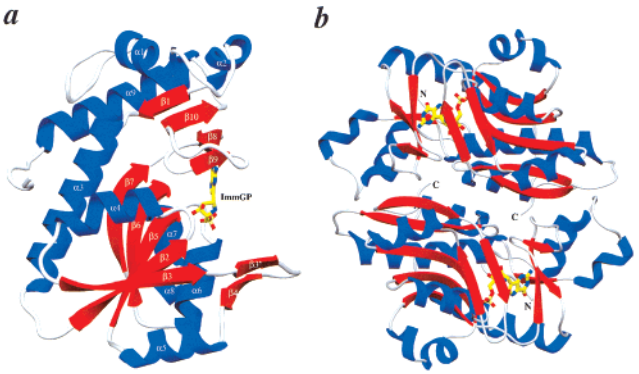

FIGURE 2: Ribbon diagrams of the *Giardia* GPRTase monomer (a) and dimer (b). The two subunits are related by a noncrystallographic 2-fold axis. In panel b, the upper and lower subunits are denoted as A and B, respectively, and are identified with this notation in the text. The N- and C-termini are labeled in panel b. This figure was generated using SETOR (*29*).

α-helices (α3, 38−56; α4, 73−81; α5, 109−117; α6, 132−140; α7, 154−159; and α8, 161−164). The segment connecting β3 and α5 (93−108, corresponding to human HGPRTase residues 102−117) has been shown to be the catalytic loop that is responsive to binding of active site ligands. In both GPRTase structures, this loop is in the open position but is ordered and forms a β-hairpin ($\beta3'$, 94−98; and β4, 103−107) secondary structure. Hydrogen bonds defining the β-hairpin are as follows: Ser95 N−O Val106, 3.2 Å; Ser95 O−N Val106, 2.8 Å; Tyr97 N−O Ser104, 2.8 Å; Try97 O−N Ser104, 2.9 Å; and Gly99 N−O Glu102, 2.9 Å. In human HGPRTase and malarial HGXPRTase complexed with immucillins and Mg·PP_i, this loop forms a similar β-hairpin in close contact with the catalytic site but is disordered in the open conformation with bound substrate (Figure 3a).

The hood subdomain (α1, α2, α9, β1, β8, β9, and β10 in Figure 2a) exhibits significant differences with respect to other HGPRTases, particularly in N-terminal and C-terminal regions (Figure 3a). In human HGPRTase, the N-terminus extends into the core subdomain and contributes a β-strand to the core domain β-sheet (*7*, *9*). In the *Giardia* GPRTase, the N-terminus folds back toward α1 (residues 10−18) and contacts a neighboring molecule related by crystallographic symmetry. The C-terminus of GPRTase is a long helix (α9, 205−222) pointing to the same side as the N-terminus and makes a significant contribution in the dimer interface (Figure 2b), while in the other HGPRTases, the equivalent α-helix is shorter and points the opposite direction in the vicinity of the catalytic loop. The small four-stranded antiparallel β-sheet (β1, 33−36; β10, 196−201; β8, 179−182; and β9, 186−188) in the center of the hood domain is similar to that of the human HGPRTase and malarial HGXPRTase (*7*, *8*). Overall, 38% of the total residues of the *Giardia* GPRTase are in α-helical structure and 28% in β-sheets, whereas in the human HGPRTase and other H/G/XPRTases, only about 27% of the total residues are in the α-helices but 33% in the β-sheets.

Dimer Interface. The *G. lamblia* GPRTase forms a dimer in the crystal structure. The subunits are related by a noncrystallographic 2-fold axis (Figure 2b). The dimer in *Giardia* is similar to those observed for the *Trypanosoma cruzi* HPRTase (*10*) and the *Tritrochomonas foetus* HGXPRTase (*11*). Although human and malarial HG(X)PRTases form tetramers in the crystal structure, the most extensive dimeric interfaces in these tetramers are similar to the dimer interfaces in *Giardia* GPRTase (*7*, *8*). The dimer interface buries 3392 $Å^2$ of total solvent accessible surface area, representing 28% of the surface area from the monomer. The dimer interface is formed by contributions from α3, β4, β9, β10, and the C-terminus from subunit A, and from β3 and α2 of subunit B. The interface is dominated by hydrophobic interactions between amino acid pairs: Phe38A and Tyr230B, Pro62A and Leu191B, Leu69A and Leu69B, Thr70A and Leu89B, Tyr73A and Phe91B, Leu74A and Val81B, and Leu191A and Thr88B. A hydrogen bond is formed between the OH of Tyr87A and the amide nitrogen of Gly194B. In addition, several water-mediated hydrogen bonds are present, including interactions between the amide nitrogen of Phe91A with OG of Thr70B, the carbonyl oxygen of Leu89A with NH_2 of Arg193B, carbonyl oxygens of Tyr87A and Gly193B, and the amide nitrogen of Leu89A with NE of Arg193B. These water-mediated hydrogen bonds are conserved in the noncrystallographically related subunits.

Giardia GPRTase·ImmucillinG Complex. The structure of *Giardia* GPRTase in complex with immucillinG was determined from the crystals that were initially grown with added immucillinGP, $MgCl_2$, and pyrophosphate. A trace activity of alkaline phosphatase (10^{-8}−10^{-7} of that of the GPRTase) converted immucillinGP to immucillinG during the crystallization process. Nucleosides are not substrates and are weak inhibitors for HGPRTases. Both independent active sites in the GPRTase·immucillinG structure revealed clear electron densities for the 9-deazaguanine portion of immucillinG. However, no density for the iminoribitol ring of the nucleoside was present. Importantly, the chemical stability of the carbon−carbon bond between 9-deazaguanine and iminoribitol ensures that the iminoribitol is present, but is disordered

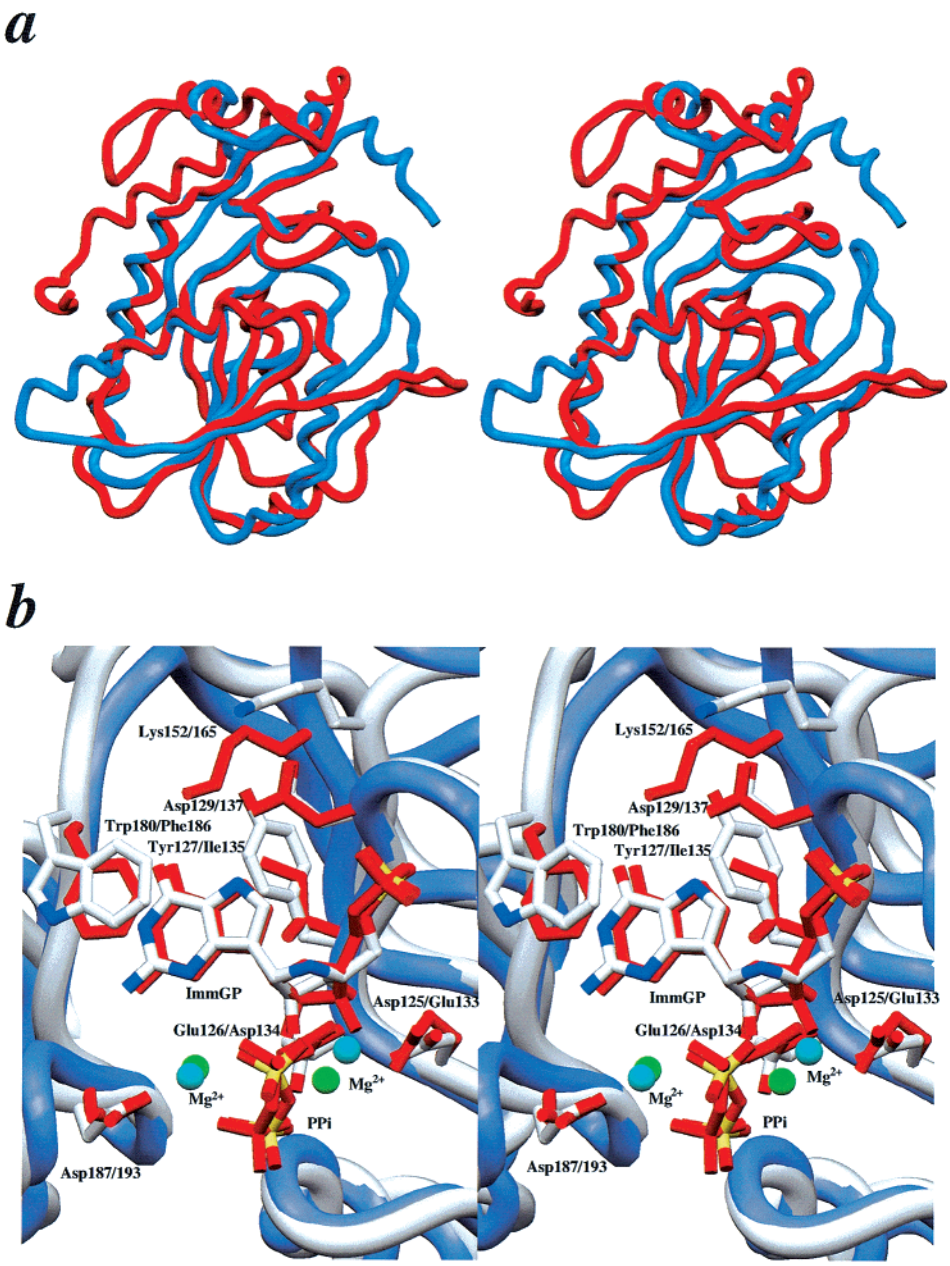

FIGURE 3: (a) Superpositions of the peptide chains from Cα atoms of the *Giardia* GPRTase·immucillinGP·Mg^{2+}·PP_i complex (red) and human HGPRTase·immucillinGP·Mg^{2+}·PP_i complex (blue). The C- and N-terminal regions of the hood domains exhibit significant differences between the two structures. (b) Superpositions of residues involved in binding and catalysis for the *Giardia* GPRTase·immucillinGP·Mg^{2+}·PP_i complex (gray, with Mg^{2+} in blue) and the human HGPRTase·immucillinGP·Mg^{2+}·PP_i complex (purple backbone, red side chains, and green Mg^{2+}). Lys165 forms a direct hydrogen bond with the exocyclic O6 of immucillinGP in the human structure, and the same Lys residue in the *Giardia* structure is 6.3 Å away from O6 of the bound inhibitor. This figure was generated using SETOR (*29*).

in the absence of the 5′-phosphate. This observation suggests that the 5′-phosphate is essential to anchor the ribosyl of substrate prior to Mg^{2+} and pyrophosphate binding. Two catalytic site acids, Asp125 and Glu126, are slightly disordered in the structure with immucillinG bound. These groups correspond to Glu133 and Asp134 in the human structure, and are involved in binding the 2′- and 3′-hydroxyl groups of immucillinGP in the fully occupied and closed catalytic sites of both human and malarial HG(X)PRTases (*7*, *8*).

The overall structures of the GPRTase·immucillinG and GPRTase·immucillinGP·Mg^{2+}·PP_i complexes are similar with rmsds for all Cα atoms of 0.3 Å. A comparison of the residues involved in ligand binding and implicated in catalysis reveals that the side chains adopt similar conformations, with the exception of Glu126, which undergoes a ∼90° rotation of the carboxyl group (Figure 4b). The 9-deazaguanine in the crystal of the enzyme·immucillinG complex is in the same position as that of bound immucillinGP in the GPRTase·immucillinGP·Mg^{2+}·PP_i structure and makes similar contacts to the enzyme. Two aromatic residues, Trp180 and Tyr127, form stacking interactions with both sides of the 9-deazaguanine, while Asp129 forms a 2.8 Å hydrogen bond with N7 of immucillinG. Asp129 (corresponding to Asp137 in human HGPRTase) has been reported to be the general acid that neutralizes the charge in the purine leaving group during transition state formation (*6*, *21*). The heterocyclic N1 and the exocyclic N2 of the 9-deazaguanine ring interact with carbonyl oxygens of Leu181 and Asp187 (corresponding to Leu187 and Asp193 in the human structure). Similar hydrogen bonding occurs with N1 and N2 of

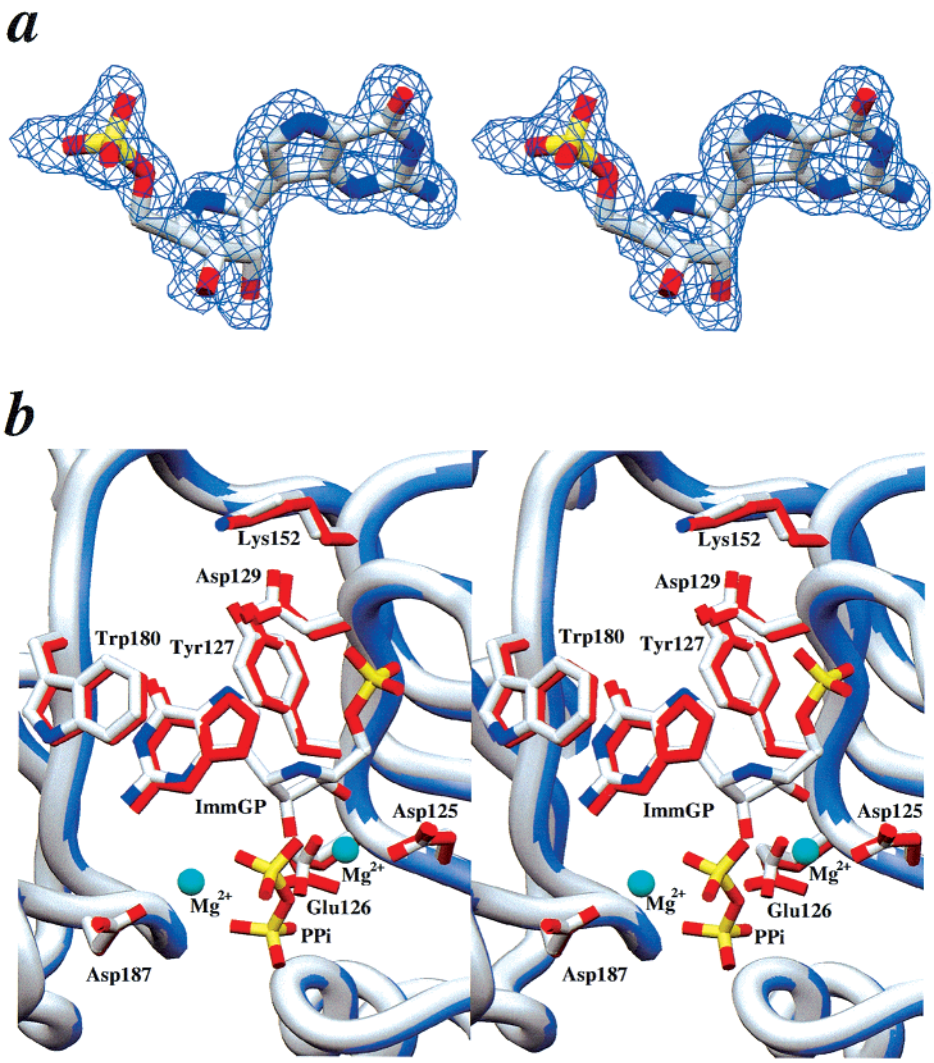

FIGURE 4: (a) Stereoview of the electron density for bound immucillinGP from the $F_o - F_c$ omit map contoured at 2.0σ. (b) Stereoview of the active site residues of the *Giardia* GPRTase·immucillinG complex (purple backbone with red side chains) compared to that of the GPRTase·immucillinGP·Mg^{2+}·PP_i complex (gray). This figure was generated using SETOR (*29*).

immucillinGP in human HGPRTase. Human and malarial complexes with immucillin 5′-phosphates and magnesium pyrophosphate reveal nine hydrogen bonds that are shorter than 3.0 Å to the nonbridging 5′-phosphoryl oxygens (*7*, *8*). Loss of these interactions for the iminoribitol group of immucillinG prevents the entire ribosyl analogue from locating an energetically favored position in the catalytic site.

ImmucillinGP Binding Site. The active site of the GPRTase·immucillinGP·Mg^{2+}·PP_i complex was fully occupied in one subunit of the dimer and partially occupied in the other. In the fully occupied active site, one immucillinGP, one pyrophosphate, and two Mg^{2+} ions were clearly present in the electron densities (e.g., Figure 4a). The second subunit gave good electron density for immucillinGP and pyrophosphate, but the magnesium ions could not be located with certainty.

The conformation of the iminoribitol ring in bound immucillinGP is significantly different from those observed in the human and malarial complexes with immucillin 5′-phosphates and Mg^{2+}·pyrophosphate (*7*, *8*). The ring adopts a 3′-endo conformation in the *Giardia* enzyme compared to a flattened 3′-exo ring in the human and malarial structures (Figure 3b). This difference is a consequence of an alteration in one of the Mg^{2+} binding sites (Figure 5 and see Mg^{2+} Binding Sites below). ImmucillinGP oxygens O2′ and O3′ do not hydrogen bond with Asp125 and Glu126 or any other protein atoms. Instead, they interact with the two acidic residues through a Mg^{2+} ion, which coordinates to the two hydroxyl groups of immucillinGP, and to Asp125 and Glu126. This contrasts with malarial HG(X)PRTase in which the equivalents of Asp125 and Glu126 form direct hydrogen bonds to the 2′- and 3′-hydroxyls (*8*).

The 5′-phosphate of immucillinGP is positioned inside a pocket formed by residues 129-DSGHT-133. The side chain and backbone atoms of residues Ser130, Gly131, and Thr133 hydrogen bond with the 5′-phosphate. As observed in the human and malarial HG(X)PRTase complexed with immucillins and Mg^{2+}·pyrophosphate, the O5′ is positioned near N4′ (2.7 Å), such that the lone pair electrons might interact with the positive charge of the iminoribitol ring ($pK_a = 6.5$) (*7*, *8*, *22*).

Substrate Specificity. Guanine is an efficient substrate for *G. lamblia* GPRTase with a K_m of 16 μM, and a k_{cat} of 77 s^{-1}, whereas hypoxanthine is a poor substrate with a K_m of 200 μM; xanthine and adenine had no detectable substrate activity at 300 μM (*5*). Therefore, the substrate specificity

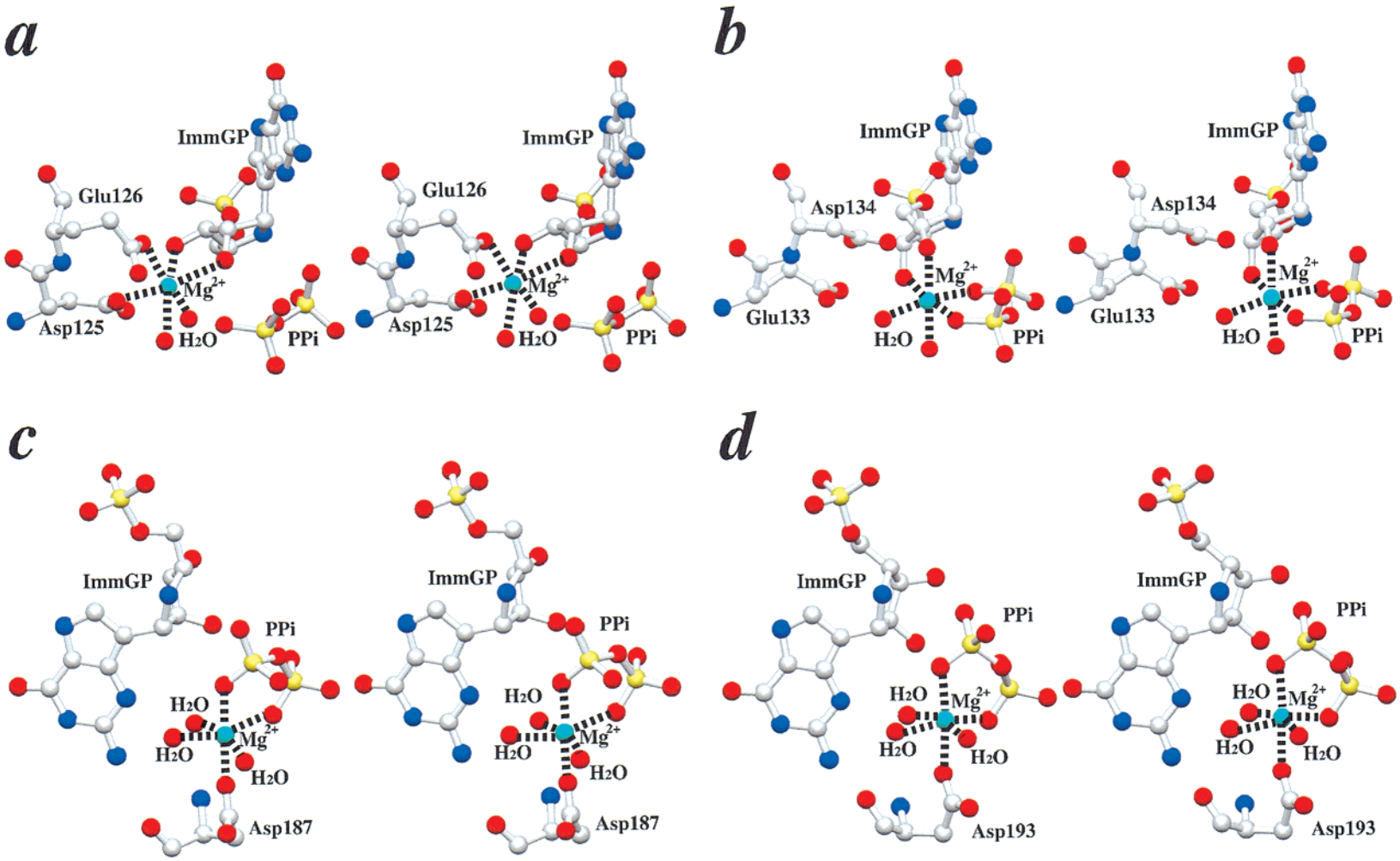

FIGURE 5: Stereoviews of the bound Mg^{2+} ions in the *Giardia* GPRTase·immucillinGP·Mg^{2+}·PP_i complex (panel a and c) and the human HGPRTase·immucillinGP·Mg^{2+}·PP_i complex (panel b and d). These structures are with the catalytic site loops open and closed, respectively. This figure was generated using SETOR (*29*).

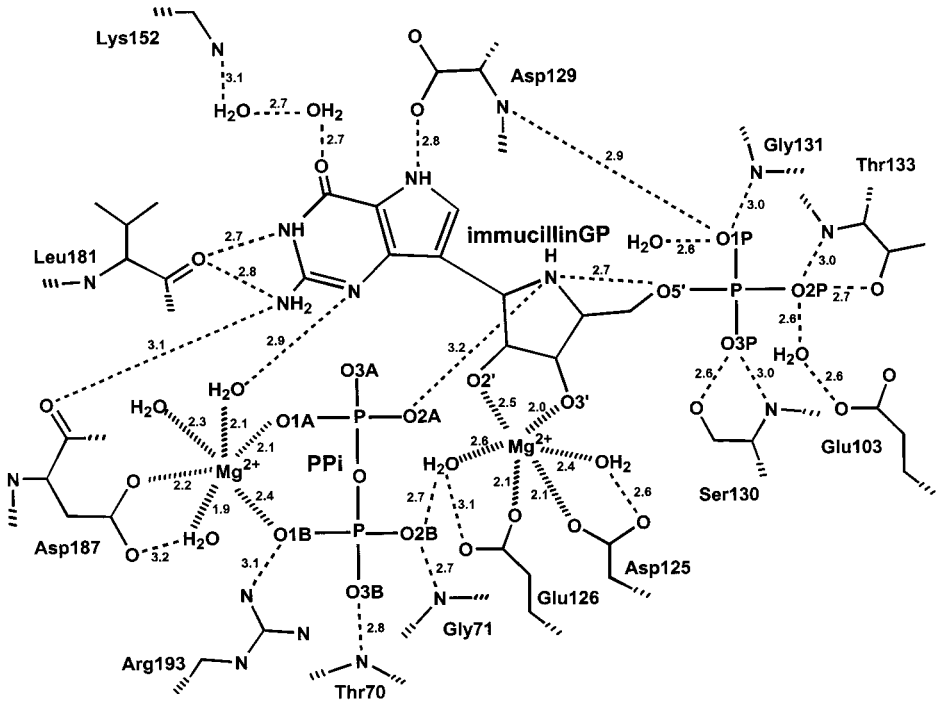

FIGURE 6: Catalytic site contacts for the *G. lamblia* GPRTase·immucillinGP·Mg^{2+}·PP_i complex, with distances in angstroms. A weakly bound water (2.6 Å) intervenes between pyrophosphate and the Mg^{2+} bound to Asp125 and Glu126. Expulsion of this water and changes in the geometry of Glu126 would permit the Mg^{2+} to chelate to O2A and O2B as seen in loop-closed complexes of HG(X)PRTases (*7*, *8*). The intervening waters between Lys152 and O6 are absent in loop-closed complexes.

of *Giardia* GPRTase is highly unique and without a parallel in known organisms.

The preference for guanine displayed by the *Giardia* enzyme is due to favorable interactions of the exocyclic amine (N2) with the backbone carbonyl oxygen of Asp181 (bifurcated hydrogen bonds being 2.7 and 2.8 Å long) and a hydrogen bond between the amine and the carbonyl of Asp187 (3.1 Å; Figure 6). Recognition of hypoxanthine in PRTases is mediated by a favorable hydrogen bond between the ϵ-amino group of a lysine and O6 of the purine ring (*7*, *8*).

The 9-deazaguanine of immucillinGP in the GPRTase complex structure is stacked between Trp180 and Tyr127 (Phe186 and Ile135 in human HGPRTase). Aromatic residues corresponding to Trp180 are conserved in all H/G/XPRTases as either a Phe or a Trp. The Tyr at position 127 is conserved in all H/G/XPRTases as either a Ile or a Leu except for the Tyr in *Giardia* GPRTase. Lys152 (Lys165 in human HGPRTase) is conserved throughout H/G/XPRTases from all species and has been reported to be important in substrate recognition in human HGPRTase. A Lys165Gln mutation in the human enzyme increased the K_m by 1000-fold (*23*). Human HGPRTase structures complexed with GMP or immucillinGP reveal Lys165 in a hydrogen bond with the 6-exocyclic oxygen of the guanine ring (see above). The same hydrogen bonding pattern was also observed in malarial HGXPRTase complexed with immucillinHP and Mg^{2+}·pyrophosphate (*8*), *T. cruzi* HPRTase complexed with formycin B and PRPP (*10*), and several other H/G/XPRTase structures determined with a substrate or an inhibitor bound. In *Giardia* GPRTase, the side chain of Lys152 is pushed away by Tyr127 which stacks against the guanine ring from the same side as the lysine (Figures 3 and 4). The distance between Nϵ of Lys152 and O6 is 6.3 Å, and this interaction is mediated by two ordered water molecules (Figure 6). The water-mediated interaction is presumably weaker than a direct hydrogen bond. The weak interaction at O6 combined with strong interactions at N2 supports the preference for guanine in the *Giardia* enzyme.

The equivalent of Leu181 is conserved throughout all H/G/XPRTases. This Leu is also important for substrate specificity in bacterial HPRTases, since the Leu to Thr mutation in this position gave a 50-fold increase in k_{cat}/K_m with guanine as a substrate (*24*). The present GPRTase structures may not fully reveal the guanine specificity, since it is possible that the position of Lys152 will change on catalytic loop closing. Similar interactions at N2 have been observed in the closed loop structure of the human HGPRTase in complex with immucillinGP, Mg^{2+}, and pyrophosphate. The malarial HGXPRTase complex structure was determined with immucillinHP, which lacks exocyclic N2, and yet the backbone and side chain atoms of these residues have conformation and hydrogen bond distances similar to those of the human HGPRTase complex with bound immucillinGP (*7*, *8*). In the vicinity of N2 of immucillinGP bound to human HGPRTase, Tyr194 and Phe198 are in hydrophobic contact with the deazaguanine ring and are highly conserved throughout all H/G/XPRTases except the *Giardia* enzyme. In *Giardia* GPRTase, the two aromatic residues are replaced with two charged amino acids, Asp188 and Arg193, and side chains of these two residues form a hydrogen bond (3.0 Å). This interaction pulls the chain segment of residues 187−189 away from N2 and C2 of the inhibitor, resulting in a hydrogen bond distance between the carbonyl oxygen of Asp187 and N2 of immucillinGP longer than that observed in the human HGPRTase·immucillinGP·Mg·PP_i complex (*7*).

Mg^{2+} Ion Coordination and Pyrophosphate Binding. Two Mg^{2+} ions were located in the filled active site of the *Giardia*

GPRTase·immucillinGP·Mg^{2+}·PP_i complex. The first Mg^{2+} ion exhibited octahedral coordination, interacting with the two acidic residues, Glu125 and Asp126 (2.1 and 2.1 Å, respectively), O3′ and O2′ of the iminoribitol ring (2.0 and 2.5 Å, respectively), and two water molecules (2.4 and 2.5 Å, respectively). This Mg^{2+} ion does not interact with pyrophosphate directly but forms a water-mediated hydrogen bond (Figure 5a).

Comparison of the Mg^{2+} binding sites with other H/G/XPRTase structures reveals that this Mg^{2+} binding mode is novel to *Giardia* GPRTase. A more distantly related glutamine phosphoribosylpyrophosphate amidotransferase has a Mg^{2+} bound in a similar position (*25*). In the human and malarial HG(X)PRTases complexed with immucillins and Mg^{2+}·pyrophosphate, a Mg^{2+} ion was involved in direct coordination with the two hydroxyl groups of the iminoribitol ring, two pyrophosphate oxygens, and two water molecules (*7*, *8*; Figure 5b). The equivalent Mg^{2+} binding site was also found in *E. coli* XPRTase complexed with Mg^{2+} and carbocyclic PRPP (*26*), *T. cruzi* HPRTase in complex with the purine analogue base from formycin B, Mg^{2+}, and PRPP (*10*), and *E. coli* glutamine phosphoribosylpyrophosphate amidotransferase (GPATase) complexed with carbocylic PRPP and Mn^{2+} (*26*). In all of these cases, there are no direct interactions between protein and this Mg^{2+} ion. In *Giardia* GPRTase, the Mg^{2+} binding site is shifted by approximately 2.5 Å away from pyrophosphate and makes direct contacts with side chain oxygens of Asp125 and Glu126. These are highly conserved amino acids in the PRPP binding motif of all PRTases (*27*). The novel position for Mg^{2+} binding in this flap open catalytic site suggests the sequence of binding events that lead to the productive loading of the active site of GPRTase: The purine ring binds, the ribosyl phosphate group is anchored by the 5′-phosphate, the first Mg^{2+} site fills without assistance from magnesium pyrophosphate, and magnesium pyrophosphate binds followed by movement of the catalytic site loop and transfer of the Mg^{2+} from Asp125 and Glu126 to form catalytically competent $(Mg^{2+})_2$·pyrophosphate. Bound pyrophosphate is sandwiched between two bidentate-chelated Mg^{2+} ions in both human and malarial HG(X)PRTases in complex with transition state analogue inhibitors and with the catalytic loops closed (*7*, *8*). The movement of this Mg^{2+} is implied by the changes shown in panels a and b of Figure 5. From the structures reported here, it is unlikely that Mg·PP_i binds prior to the free Mg^{2+}, since Mg·PP_i binding reduces the solvent accessible area for bound Mg^{2+} from 24 to 4 Å.

The second Mg^{2+} ion bound in the active site in GPRTase·immucillinGP·Mg^{2+}·PP_i complex forms a symmetric, bidentate interaction with pyrophosphate (Figure 5c). This binding motif is also observed in the human and malarial HG(X)PRTases in complex with immucillins (*7*, *8*; Figure 5d), and *T. cruzi* HPRTase in complex with formycin B and PRPP (*10*). The Mg^{2+} ion coordinates with two oxygens of pyrophosphate (2.0 and 2.4 Å, respectively), three water molecules (1.9, 2.1, and 2.4 Å, respectively), and a side chain oxygen of Asp187 (2.1 Å). Asp187 is the only amino acid in contact with this Mg^{2+} ion. Mutation at this position (Asp193) results in the human genetic defect Lesch-Nyhan syndrome (*28*).

Pyrophosphate is positioned beneath the bound immucillinGP. The phosphoryl group distal to the inhibitor hydrogen bonds with the backbone amide nitrogens of Thr70 and Gly71, and the side chain of Arg193. In both structures of GPRTase, Thr70 is identified as a cis peptide. This geometry positions the amide nitrogen of Thr70 toward the pyrophosphate binding site, promoting a hydrogen bond when pyrophosphate is bound. The *cis* peptide at this location has been observed in human and malarial HG(X)PRTases complexed with immucillins (*7*, *8*), in *T. cruzi* HPRTase (*10*), and in *E. coli* XPRTase (*25*). The enzymatically reactive phosphoryl of pyrophosphate interacts with N4′ of immucillinGP (3.2 Å), and a negatively charged pyrophosphate oxygen is proposed as one of the stabilizing factors for transition state formation. The tight binding of iminoribitol analogues indicates that the reaction proceeds through formation of ribooxycarbenium ion, and the negatively charged oxygen stabilizes the positive charge of the transition state (*6*−*8*, *22*).

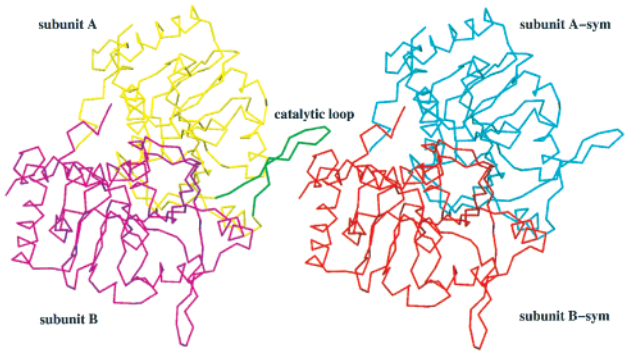

FIGURE 7: Dimer crystal packing for the *G. lamblia* GPRTase·immucillinGP·Mg^{2+}·PP_i complex showing two dimers. The yellow and magenta dimer on the left interacts with the dimer on the right through the catalytic loop of left subunit A (shown in green). This contact is the closest contact between the dimers in this plane, and therefore constitutes a crystal lattice interaction. Each A/B pair represents an asymmetric unit, and the two A/B pairs are symmetrically related units. Four pairs of hydrogen bonds are located between the loop and its neighbor at the crystal lattice interface. They include the following: (1) the amide nitrogen of Thr100A with the carbonyl oxygen of Val5B-sym (2.9 Å), (2) the amide nitrogen of Glu102A with the carbonyl oxygen of Thr6B-sym (3.0 Å), (3) the NH_2 of Arg101A with the carbonyl oxygen of Tyr23A-sym (2.9 Å), and (4) the OH of Tyr97A with the carbonyl oxygen of Ser4B-sym (2.6 Å). This figure was generated using SETOR (*29*).

Catalytic Loop Domain. The tip of the catalytic loop in the *Giardia* GPRTase·immucillinGP·Mg^{2+}·PP_i complex is in the open position, and is well ordered in the subunit with the fully occupied active site. Close contacts with the neighboring molecule in the crystal lattice order the loop and prevent it from closing over the active site (Figure 7). The body of the catalytic loop forms a two-stranded antiparallel β-secondary structure (residues 94−98 and 103−107) and four hydrogen bonds to the crystallographically related neighboring subunit. Even though the tip of the catalytic loop is in the open position, the body of the loop stays close to the active site and side chains of some amino acids point toward the inhibitor. For example, Glu133 forms a water-mediated hydrogen bond with the 5′-phosphate of the bound immucillinGP.

Conclusions. Crystallization of GPRTase from *G. lamblia* with partially filled catalytic sites, followed by crystal soaks with the transition state analogue components, has stabilized unusual phosphoribosyltransferase conformations that are

postulated to occur prior to catalytic site closing and formation of the stabilized transition state complex. The structures of GPRTase·immucillinG and GPRTase·immucillinGP·Mg^{2+}·PP_i complexes represent early steps on the path between empty catalytic sites and formation of the transition state conformation. These structures provide sufficient structural information for proposing the sequence of binding events that lead from the empty catalytic site to the formation of the transition state.

REFERENCES

1. National Institute of Allergy and Infectious Diseases, Giardiasis Fact Sheet (1998) U.S. Department of Health of Human Services.
2. Despommier, D. D., Gwadz, R. W., and Hotez, P. J. (1994) in *Parasitic Diseases*, 3rd ed., pp 144−149, Springer-Verlag, New York.
3. Wang, C. C., and Aldritt, S. M. (1984) Purine salvage networks in *Giardia lamblia*, *J. Exp. Med. 158*, 1703−1712.
4. Sommer, J. M., Ma, H., and Wang, C. C. (1996) Cloning, expression and characterization of an unusual guanine phosphoribosyltransferase from *Giardia lamblia*, *Mol. Biochem. Parasitol. 78*, 185−193.
5. Page, J. P., Munagala, N. R., and Wang, C. C. (1999) Point mutations in the guanine phosphoribosyltransferase from *Giardia lamblia* modulate pyrophosphate binding and enzyme catalysis, *Eur. J. Biochem. 259*, 565−571.
6. Li, C. M., Tyler, P. C., Furneaux, R. H., Kicska, G., Xu, Y., Grubmeyer, C., and Schramm, V. L. (1999) Transition state inhibitors for human and malarial hypoxanthine-guanine phosphoribosyltransferase, *Nat. Struct. Biol. 6*, 582−587.
7. Shi, W., Li, C. M., Tyler, P. C., Furneaux, R. H., Grubmeyer, C., Schramm, V. L., and Almo, S. C. (1999) The 2.0 Å structure of human hypoxanthine-guanine phosphoribosyltransferase in complex with a transition-state analog inhibitor, *Nat. Struct. Biol. 6*, 588−593.
8. Shi, W., Li, C. M., Tyler, P. C., Furneaux, R. H., Cahill, S. M., Girvin, M. E., Grubmeyer, C., Schramm, V. L., and Almo, S. C. (1999) The 2.0 Å structure of malarial purine phosphoribosyltransferase in complex with a transition-state analogue inhibitor, *Biochemistry 38*, 9872−9880.
9. Eads, J. C., Scapin, G., Xu, Y., Grubmeyer, C., and Sacchettini, J. C. (1994) The crystal structure of human hypoxanthine-guanine phosphoribosyl-transferase with bound GMP, *Cell 78*, 325−334.
10. Focia, P. J., Craig, S. P., III, and Eakin, A. E. (1998) Approaching the transition state in the crystal structure of a phosphoribosyltransferase, *Biochemistry 37*, 17120−17127.
11. Somoza, J. R., Chin, M. S., Focia, P. J., Wang, C. C., and Fletterick, R. J. (1996) Crystal structure of the hypoxanthine-guanine-xanthine phosphoribosyl-transferase from the protozoan parasite *Tritrichomonas foetus*, *Biochemistry 35*, 7032−7040.
12. Schumacher, M. A., Carter, D., Roos, D. S., Ullman, B., and Brennan, R. G. (1996) Crystal structures of *Toxoplasma gondii* HGXPRTase reveal the catalytic role of a long flexible loop, *Nat. Struct. Biol. 3*, 881−887.
13. Morrison, J. F., and Walsh, C. T. (1988) The significance and behavior of slow-binding enzyme inhibitors, *Adv. Enzymol. 61*, 201−301.
14. Otwinowski, Z., and Minor, W. (1997) Processing of X-ray diffraction data collected in oscillation mode, *Methods Enzymol. 276*, 307−326.
15. Terwilliger, T. C., and Berendzen, J. (1999) Automated structure solution for MIR and MAD, *Acta Crystallogr. D55*, 849−861.
16. Collaborative Computational Project, Number 4 (1994) *Acta Crystallogr. D50*, 70−763.
17. Kleywegt, G. J., and Read, R. J. (1997) Not your average density, *Structure 5*, 1557−1569.
18. Jones, T. A. (1985) Interactive computer program graphics: Frodo, *Methods Enzymol. B115*, 157−171.
19. Brunger, A. T., et al. (1998) Crystallography & NMR System, *Acta Crystallogr. D54*, 905−921.
20. Laskowski, R. A., MacArthur, M. W., and Thorton, J. M. (1993) PROCHECK: a program to check the stereochemical quality of protein structures, *J. Appl. Crystallogr. 26*, 283−291.
21. Xu, Y., and Grubmeyer, C. (1998) Catalysis in human hypoxanthine-guanine phosphoribosyltransferase: Asp-137 acts as a general acid/base, *Biochemistry 37*, 4114−4124.
22. Horenstein, B. A., and Schramm, V. L. (1993) Correlation of the molecular electrostatic potential surface of an enzymatic transition state with novel transition-state inhibitors, *Biochemistry 32*, 9917−9925.
23. Xu, Y., Eads, J., Sacchettini, J. C., and Grubmeyer, C. (1997) Kinetic mechanism of human hypoxanthine-guanine phosphoribosyltransferase: rapid phosphoribosyl transfer chemistry, *Biochemistry 36*, 3700−3712.
24. Sydney, C. C., Craig, S. P., III, and Eakin, A. E. (1998) A single amino acid substitution in the human and a bacterial hypoxanthine phosphoribosyltransferase modulates specificity for the binding of guanine, *Biochemistry 37*, 3491−3498.
25. Krahn, J. M., Kim, J. H., Burns, M. R., Parry, R. J., Zalkin, H., and Smith, J. L. (1997) Coupled formation of an amidotransferase interdomain ammonia channel and a phosphoribosyltransferase active site, *Biochemistry 36*, 11061−11068.
26. Vos, S., Parry, R. J., Burns, M. R., de Jersey, J., and Martin, J. L. (1998) Structures of free and complexed forms of *Escherichia coli* xanthine-guanine phosphoribosyltransferase, *J. Mol. Biol. 282*, 875−889.
27. Hove-Jensen, B., Harlow, K. W., King, C. J., and Switzer, R. L. (1986) Phosphoribosylpyrophosphate synthetase of *Escherichia coli*: properties of the purified enzyme and primary structure of the *prs* gene, *J. Biol. Chem. 267*, 6765−6771.
28. Wilson, J. M., Stout, J. T., Palella, T. D., Davidson, B. L., Kelley, W. N., and Caskey, C. T. (1986) A molecular survey of hypoxanthine-guanine phosphoribosyltransferase deficiency in man, *J. Clin. Invest. 77*, 188−195.
29. Evan, S. V. (1993) SETOR: hardware lighted three-dimensional solid model representation of macromolecules, *J. Mol. Graphics 11*, 134−138.

BI000128T